

## The pH Titration Study of Lithium Ion Adsorption on $\lambda$ -MnO<sub>2</sub>

Kenta Ooi,\* Yoshitaka MIYAI, Shunsaku KATO, Hiroshi MAEDA,<sup>†</sup> and Mitsuo ABE<sup>††</sup>

Government Industrial Research Institute, Shikoku, 2-3-3 Hananomiya-cho, Takamatsu 761

<sup>†</sup>Department of Chemistry, Faculty of Science, Nagoya University, Furo-cho, Chikusa-ku, Nagoya 464

<sup>††</sup>Department of Chemistry, Faculty of Science, Tokyo Institute of Technology, 2-12-1, Ookayama, Meguro-ku 152  
(Received June 18, 1987)

The pH titration curves of  $\lambda$ -MnO<sub>2</sub> showed apparently dibasic acid character toward Li<sup>+</sup> ions, but a monobasic acid character toward Na<sup>+</sup>, K<sup>+</sup>, Rb<sup>+</sup>, and Cs<sup>+</sup> ions. The adsorptive capacities of alkali metal ions increased in the order; K<sup>+</sup>, Rb<sup>+</sup>, Cs<sup>+</sup> < Na<sup>+</sup> < Li<sup>+</sup> at pH 10. Overall equilibrium constants were calculated by a simplified Gaines-Thomas equation from the titration curves based on the ion-exchange mechanism. Thermodynamic data were derived for the system of (0.1-M LiCl+LiOH)(1 M=1 mol dm<sup>-3</sup>) at different temperatures. Effects of ionic strength and adsorption temperature on the lithium ion adsorptivity were studied using (LiCl+LiOH) and (KCl+LiOH) solutions.

Ion-sieve type manganese oxides show excellent selectivities for certain ions or group of ions.<sup>1-7)</sup> They are prepared by a crystallization of manganese hydroxide containing metal ions, followed by a topotactic extraction of the metal ions with mineral acid. Their adsorptive properties depend on the kind of metal ions introduced as precursors into the manganese hydroxide.<sup>2,6)</sup> When lithium and magnesium ions were used as introducing ions, the manganese oxides obtained show a remarkably high selectivity for lithium ions.<sup>6,7)</sup> Their lithium-selective properties are closely related to the formation of such spinel-type materials as LiMn<sub>2</sub>O<sub>4</sub> and MgMn<sub>2</sub>O<sub>4</sub> during thermal crystallization while being prepared.

Recently, Hunter prepared spinel-type manganese oxide ( $\lambda$ -MnO<sub>2</sub>) by extracting lithium from pure LiMn<sub>2</sub>O<sub>4</sub> with acid.<sup>8)</sup> Because of its uniform character,  $\lambda$ -MnO<sub>2</sub> is very suitable as a model compound for a fundamental study of the ion-sieve effect for metal ions extracted from the aqueous phase. In a previous paper, its adsorptive properties for various metal ions showed a remarkably high selectivity for lithium ions in a range above pH 2.5.<sup>9)</sup> The metal-ion uptake at pH 10 reached about 5 meq·g<sup>-1</sup> for lithium ions but less than 0.2 meq·g<sup>-1</sup> for potassium and cesium ions. The distribution coefficients (*K<sub>d</sub>*'s) of metal ions at pH 4 were in the order Na<sup>+</sup> < K<sup>+</sup> < Rb<sup>+</sup> < Cs<sup>+</sup> < Li<sup>+</sup> for alkali metal-, Mg<sup>2+</sup> < Ca<sup>2+</sup> < Sr<sup>2+</sup> < Ba<sup>2+</sup> for alkaline earth metal-, and Ni<sup>2+</sup> < Zn<sup>2+</sup> < Co<sup>2+</sup> < Cu<sup>2+</sup> for transition metal-ions. These results are readily explained if we recognize that the tetrahedral vacant sites in  $\lambda$ -MnO<sub>2</sub> are too narrow for metal ions other than lithium to enter. The only species which can enter these sites are H<sup>+</sup> and dehydrated Li<sup>+</sup> ions.

The present paper describes a pH titration study on  $\lambda$ -MnO<sub>2</sub> for alkali metal ions. The selectivity constants and overall thermodynamic constant were evaluated from the titration data based on the ion-exchange model. Acid-base properties have been investigated for different types of manganese oxides from electrochemical<sup>10,11)</sup> and geochemical<sup>12-14)</sup> interests and for the fundamental study of the adsorption

phenomena.<sup>15,16)</sup>

### Experimental

**Ion-Exchange Material and Characterization.** The  $\lambda$ -MnO<sub>2</sub> used was the same as that described in a preceding paper.<sup>8)</sup> It was prepared by the acid treatment of LiMn<sub>2</sub>O<sub>4</sub> with a 1-M HNO<sub>3</sub> solution. The lithium content of the acid-treated sample was 0.12 meq·g<sup>-1</sup>, indicating that more than 97% of the lithium was extracted from the LiMn<sub>2</sub>O<sub>4</sub> by the acid treatment. A powdered X-ray diffraction analysis showed  $\lambda$ -MnO<sub>2</sub> of a spinel type structure with an 0.800-nm lattice constant on a cubic unit cell.

**pH Titration Curve.** A weighed amount (0.100 g) of the  $\lambda$ -MnO<sub>2</sub> was immersed into a mixed solution (10 cm<sup>3</sup>) of (MCl+MOH) (M=Li, Na, K, Rb, Cs) in varying ratios with intermittent shaking at 25 °C. The concentration of MCl was adjusted to 0.1 M. After shaking for 3 weeks, the pH of the supernatant solution was determined in a decarbonated atmosphere. The kinetic study showed that three weeks were sufficient to attain a constant pH value. The metal ion concentration in the supernatant solution was determined by atomic absorption spectrometry. The metal ion uptake by  $\lambda$ -MnO<sub>2</sub> was evaluated from the difference between the initial and equilibrium concentrations of the metal ion in the solution or from determining metal ions after dissolving metal ion-adsorbed  $\lambda$ -MnO<sub>2</sub> with a mixed solution of concentrated HNO<sub>3</sub> and HCl. The chloride ion uptake was determined by ion chromatography after dissolving the  $\lambda$ -MnO<sub>2</sub> with a mixed solution of H<sub>2</sub>O<sub>2</sub> and H<sub>2</sub>SO<sub>4</sub>.

In the case of lithium ion adsorption, the effects of ionic strength and adsorption temperature were examined in (KCl+LiOH) and (LiCl+LiOH) systems in addition to the above titration.

**Apparatus.** X-Ray diffraction analysis was carried out with a Rigaku Denki X-ray diffractometer (model Rad II) using Ni filtered Cu K $\alpha$  radiation (graphite monochromator). A Perkin-Elmer atomic absorption spectrophotometer (model 403) was employed for atomic absorption spectrometry and a Horiba M8s pH meter for pH measurement. A Dionex Ion Chromatograph apparatus (model 10) was used for ion chromatography.

**Reagents.** All the chemicals were of an analytical grade from Wako Pure Chemical Ind. Ltd., except for RbCl, RbOH, and CsOH which were obtained from Merck Ltd. These were used without further purification.

## Results and Discussion

**pH Titration Curves.** The pH titration curves and pH dependences of metal ion uptakes are shown in Fig. 1. A remarkable difference was obtained between a (LiCl+LiOH) system and the other metal salt systems on the pH titration curve. The pH titration curve in the (LiCl+LiOH) system (Fig. 1, top right) showed a dibasic acid character. The apparent capacity of  $\text{Li}^+$  was found to be about  $5 \text{ meq} \cdot \text{g}^{-1}$  on the pH titration curve. The supernatant solutions at  $\text{pH} > 8$  had a slightly purplish color due to the presence of a small amount of  $\text{Mn(VII)}$  ions. Their concentration was less than  $5 \times 10^{-4} \text{ M}$  by atomic absorption spectrometry. Smaller differences than the Li-system were observed between the pH titration curves for the other systems and for the blank experiment. A small apparent capacity of  $0.2 \text{ meq} \cdot \text{g}^{-1}$  was obtained even on the system of (NaCl+NaOH). The supernatant solutions were colorless over the pH ranges studied.

The apparent capacities determined by metal ion uptakes were nearly equal to those obtained by the differences between the blank run and each titration curve (Fig. 1(B)). This suggests that the metal ion adsorption proceeds by an ion-exchange mechanism. The apparent adsorptive capacity increased in the

order:  $\text{Na}, \text{K}, \text{Rb}, \text{Cs} \ll \text{Li}$  at pH values below 7. The affinity order changed to  $\text{K}, \text{Rb}, \text{Cs} < \text{Na} \ll \text{Li}$  above pH 7, probably due to the large steric effect for large unhydrated cations (K, Rb, Cs) at higher pH. The chloride ion uptakes were found to be less than  $0.01 \text{ meq} \cdot \text{g}^{-1}$  over the pH range studied. The affinity orders in the present study showed large differences from those on other types of manganese oxides. For example, cryptomelane-type hydrous manganese(IV) oxide (CRYMO) shows the affinity orders;  $\text{Li} < \text{Na} < \text{Cs} < \text{Rb} < \text{K}$  at pH 2 and  $\text{Cs} < \text{Rb} < \text{Na} < \text{Li} < \text{K}$  at pH 10,<sup>16)</sup> and the layered hydrous manganese oxide ( $\text{H}_4\text{Mn}_9\text{O}_{18} \cdot 7\text{H}_2\text{O}$ )  $\text{Li} < \text{Na} < \text{K}$  at  $\text{pH} < 4$  and  $\text{K} < \text{Na} < \text{Li}$  at  $\text{pH} > 5$ .<sup>5)</sup>

The difference in the affinity order between  $\lambda\text{-MnO}_2$  and CRYMO can well be understood based on the difference in crystal structure. Cryptomelane-type manganese oxide has  $[2 \times 2]$  tunnels of edge-shared  $\text{MnO}_6$  octahedra.<sup>17)</sup> Tsuji and Abe have pointed out that these  $[2 \times 2]$  tunnels are very suitable to fix the metal ions with an effective ionic radius of 0.14 nm ( $\text{K}^+, \text{Rb}^+, \text{Ba}^{2+}$ ).<sup>4)</sup> Our result agrees in showing that the manganese oxides with  $[2 \times 2]$  tunnels have high selectivities for  $\text{Rb}^+$  and  $\text{K}^+$  ions.<sup>6)</sup> The  $\lambda\text{-MnO}_2$  in  $\text{H}^+$  form can be derived from the spinel structure of  $\text{LiMn}_2\text{O}_4$ .<sup>18)</sup> The cubic  $\text{LiMn}_2\text{O}_4$  spinel (lattice parameter  $a_0$ ) contains eight formula units and has its close-packed array of

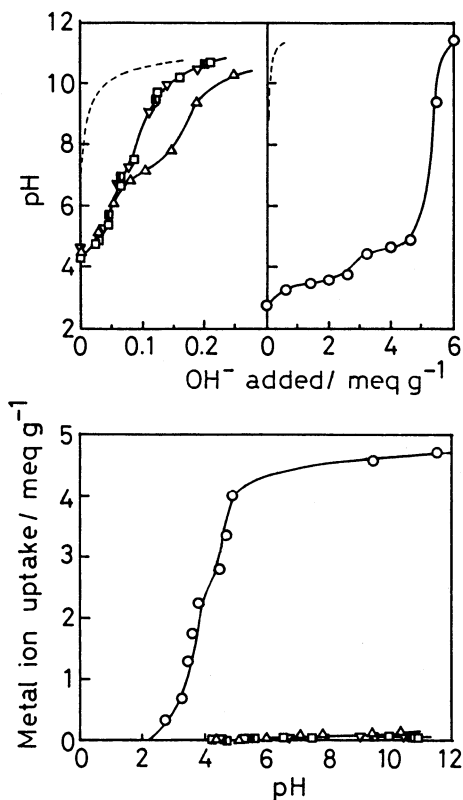


Fig. 1. pH titration curves of  $\lambda\text{-MnO}_2$  by various bases and the pH dependences of metal ion uptake.  $\lambda\text{-MnO}_2$ : 0.100 g, soln: (0.1-M  $\text{MCl} + \text{MOH}$ ) ( $\text{M} = \text{Li}(\bigcirc), \text{Na}(\triangle), \text{K}(\square), \text{Rb}(\nabla), \text{Cs}(\blacksquare)$ ), total vol. of soln:  $10 \text{ cm}^3$ , temp:  $25^\circ\text{C}$ . The dotted lines describe blank titrations.

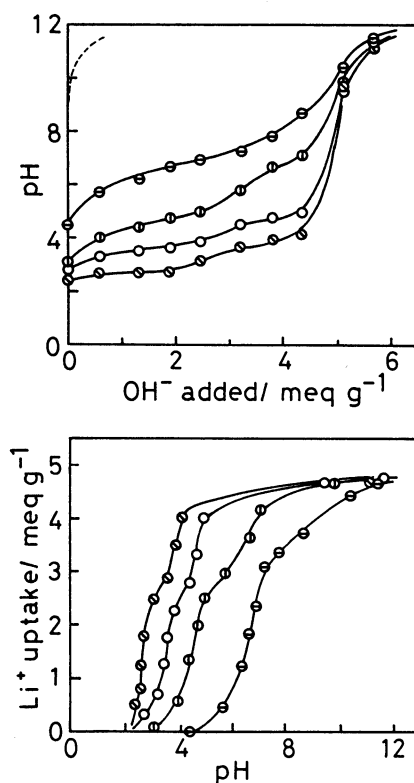


Fig. 2. pH titration curves of  $\lambda\text{-MnO}_2$  toward lithium ions and the pH dependences of lithium ion uptakes.  $\lambda\text{-MnO}_2$ : 0.100 g, soln: ( $\text{LiCl} + \text{LiOH}$ ) (concn of  $\text{LiCl}$ : 0 M( $\bigcirc$ ), 0.01 M( $\diamond$ ), 0.1 M( $\bigcirc$ ), 1 M( $\square$ )), total vol. of soln:  $10 \text{ cm}^3$ , temp:  $25^\circ\text{C}$ .

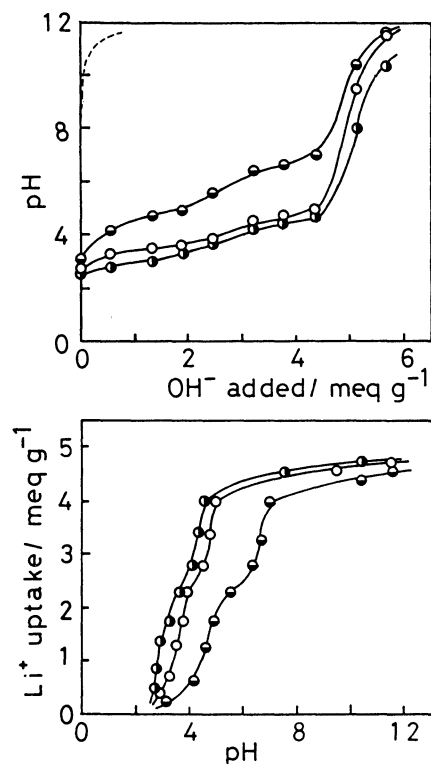


Fig. 3. pH titration curves in (0.1-M  $\text{LiCl}+\text{LiOH}$ ) solution and the pH dependences of lithium ion uptakes. The experimental conditions are the same as those in Fig. 2 except for adsorption temperature. Temp: 10°C (●), 25°C (○), 40°C (●).

oxygens located at the 32e positions of the space group  $\text{Fd}3\text{m}(\text{O}_h^7)$ .<sup>19)</sup> The  $\text{Mn}^{3+}$  and  $\text{Mn}^{4+}$  ions occupy half the octahedral sites, and the  $\text{Li}^+$  ions an eighth of the tetrahedral sites. The acid treatment of  $\text{LiMn}_2\text{O}_4$  causes the removal of nearly all of the lithium from the tetrahedral sites while maintaining a spinel structure.<sup>8)</sup> Therefore,  $\lambda\text{-MnO}_2$  has a structure that is related to spinel but with vacant tetrahedral sites. Since the size of the vacant sites is markedly smaller than the width of the  $[2\times 2]$  tunnels, it is reasonable to consider that the vacant sites are too narrow to hold the alkali metal ions except lithium even in a dehydrated state. Therefore, the pH titration curves for  $\text{Na}^+$ ,  $\text{K}^+$ ,  $\text{Rb}^+$ , and  $\text{Cs}^+$  ions suggests that the ion-exchange reactions proceed only at the surface of the  $\lambda\text{-MnO}_2$  particles.

**The pH Titration Curves in ( $\text{LiCl}+\text{LiOH}$ ) Solutions.** Figure 2 illustrates the pH titration curves in ( $\text{LiCl}+\text{LiOH}$ ) solutions with different  $\text{LiCl}$  concentrations. The pH titration curve shifts to lower pH range with increasing  $\text{LiCl}$  concentration. Figure 3 showed that the titration curve shifted to lower pH range with increasing adsorption temperature in the system of the (0.1-M  $\text{LiCl}+\text{LiOH}$ ). The maximum lithium ion uptake can be estimated to be  $4.75 \text{ meq} \cdot \text{g}^{-1}$  from Figs. 2 and 3, which is somewhat smaller than the value that is expected from the chemical formula of  $\text{LiMn}_2\text{O}_4$  ( $5.7 \text{ meq} \cdot \text{g}^{-1}$ ).

The previous paper indicated that the lattice con-

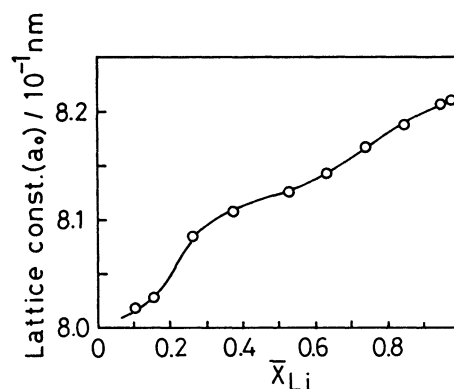


Fig. 4. Lattice constant of spinel structure as a function of  $\bar{X}_{\text{Li}}$ . Ion-exchanged  $\lambda\text{-MnO}_2$  are obtained from (1-M  $\text{LiCl}+\text{LiOH}$ ) solution at 25°C.

stant ( $a_0$ ) of the spinel structure increased by adsorption of lithium ions.<sup>9)</sup> A similar tendency was also observed in the present study. The  $a_0$  value calculated from the  $d_{111}$  peak of the X-ray diffraction pattern is plotted against  $\bar{X}_{\text{Li}}$  ( $\bar{X}_{\text{Li}}$  in Fig. 4: Equivalent fraction of lithium ions in  $\lambda\text{-MnO}_2$ =lithium ion uptake/maximum lithium ion uptake). There was a difference in  $a_0$  vs.  $\bar{X}_{\text{Li}}$  curves between  $\bar{X}_{\text{Li}} < 0.5$  and  $\bar{X}_{\text{Li}} > 0.5$ . The curve was sigmoidal at  $\bar{X}_{\text{Li}} < 0.5$  with steep slope around  $\bar{X}_{\text{Li}}=0.25$ . The  $a_0$  value increased gradually with increasing  $\bar{X}_{\text{Li}}$  in a range of  $\bar{X}_{\text{Li}} > 0.5$ . The lithium ion uptake vs. pH curves (Fig. 2) showed a pH rise at the boundary of the two curves ( $\bar{X}_{\text{Li}}=0.5$ ). These results suggest that the mode of the insertion reaction of lithium ions differed slightly between  $\bar{X}_{\text{Li}} < 0.5$  and  $\bar{X}_{\text{Li}} > 0.5$ . The presence of a stable  $\text{Li}_{0.5}\text{Mn}_2\text{O}_4$  species has been observed in the case of the electrochemical removal of lithium from  $\text{LiMn}_2\text{O}_4$ ; the removal of lithium proceeds easily to  $\text{Li}_{0.5}\text{Mn}_2\text{O}_4$  but further electrochemical extraction becomes more difficult.<sup>19)</sup>

**The pH Titration Curves in ( $\text{KCl}+\text{LiOH}$ ) Solutions.** Figure 5 illustrates pH titration curves in ( $\text{KCl}+\text{LiOH}$ ) solutions with different  $\text{KCl}$  concentrations. The pH titration curve and the lithium ion uptake curve were scarcely influenced by the addition of  $\text{KCl}$  in a range below pH 7. This indicates that the sites for lithium ion adsorption are very specific and are scarcely influenced by the presence of potassium ions. In the range above pH 7, the pH titration curve showed a tendency to shift to lower pH values by the addition of  $\text{KCl}$ , and the lithium ion uptake to increase. The increase of the lithium ion uptake may not be due to a  $\text{Li}^+-\text{K}^+$  exchange, because the lithium ion uptake decreases with  $\text{KCl}$  concentration in the case of competing exchange between lithium and potassium ions. The pH titration curves suggest that the  $\lambda\text{-MnO}_2$  has negative charge at  $\text{pH} > 5$ . Therefore, both the decrease of the pH value and the increase of the lithium ion uptake may be due to a decrease of the negative potential at the surface of  $\lambda\text{-MnO}_2$  by the addition of  $\text{KCl}$ . The decrease of pH with increasing

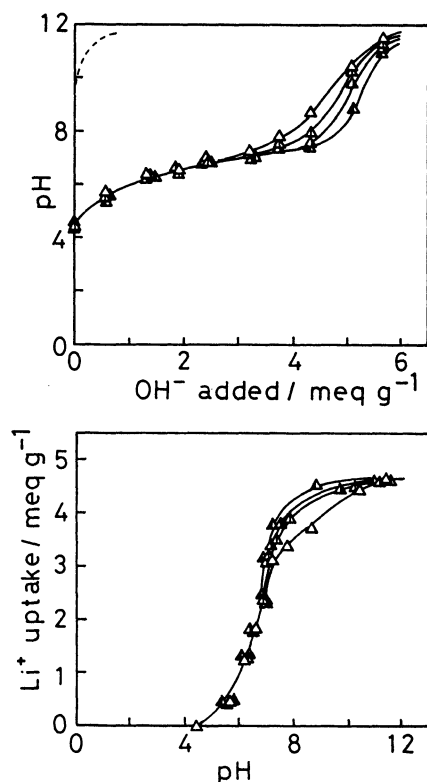
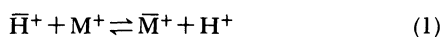


Fig. 5. pH titration curves in (KCl+LiOH) solutions and the pH dependences of lithium ion uptakes. The experimental conditions are the same as those in Fig. 2 except for KCl concentration. KCl concn: 0 M( $\Delta$ ), 0.03 M( $\square$ ), 0.1 M( $\circ$ ), and 1 M( $\blacktriangle$ ).

salt concentration usually occurs in aqueous phase for negatively charged metal oxides owing to a decrease of the surface negative charge.<sup>14,20)</sup>

**Analysis Based on the Model of Ion-Exchange Reaction.** The pH titration data can be analyzed on the basis of the ion-exchange mechanism as follows,



where bar refers to  $H^+$  or  $M^+$  in  $\lambda$ -MnO<sub>2</sub> and  $M^+$  is monovalent alkali metal ions. The equilibrium constant,  $K$ , of the above reaction is defined as,

$$K = [a_H(\bar{f}_M \bar{X}_M)] / [a_M(\bar{f}_H \bar{X}_H)] = K_C(\bar{f}_M / \bar{f}_H) \quad (2)$$

where  $a_H$  and  $a_M$  are activities of protons and metal ions in solution, respectively,  $\bar{X}_H$  and  $\bar{X}_M$  are the equivalent fractions of  $H^+$  and  $M^+$  in the  $\lambda$ -MnO<sub>2</sub>, respectively, and  $\bar{f}_H$  and  $\bar{f}_M$  are the activity coefficients of  $H^+$  and  $M^+$  in the  $\lambda$ -MnO<sub>2</sub> phase, respectively.  $K_C$  is the selectivity constant including the activity coefficient of the metal ions in solution. It can be evaluated from the pH titration data as follows,

$$\begin{aligned} pK_C = -\log K_C &= -\log [(a_H \bar{X}_M) / (a_M \bar{X}_H)] \\ &= pH - \log [\bar{X}_M / (1 - \bar{X}_M)] + \log a_M. \end{aligned} \quad (3)$$

In the case of a uni-univalent ion-exchange system, the contribution of the activity coefficient term in aqueous solution does not deviate seriously even over a temper-

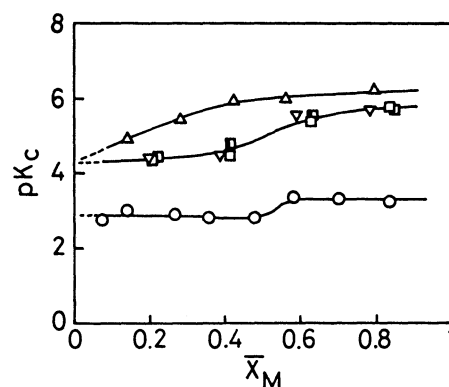


Fig. 6.  $pK_c$  vs.  $\bar{X}_M$  plots calculated from Fig. 1. The symbols are the same as those in Fig. 1.

ature range from 283 to 313 K. Therefore, Eq. 3 can be related to the concentration term of metal ions ( $C_M$ ) of Eq. 4,

$$pK_c \doteq pH - \log [\bar{X}_M / (1 - \bar{X}_M)] + \log C_M. \quad (4)$$

The  $K$  value and standard free energy change ( $\Delta G^\circ$ ) can be evaluated by using the simplified treatment of the Gaines-Thomas equation, assuming that the change of water content in the exchanger and the entrance of anion from the solution phase are negligible,<sup>21)</sup>

$$pK = -\log K = \int_0^1 pK_c d\bar{X}_M \quad (5)$$

$$\Delta G^\circ = (2.303 RT) pK \quad (6)$$

**$pK_c$  vs.  $\bar{X}_M$  Plots.** Figure 6 illustrates a plot of  $pK_c$  vs.  $\bar{X}_M$  in (MCl+MOH) system using Eq. 4. The maximum uptakes ( $\bar{X}_M = 1$ ) of the metal ions were estimated as 4.75 meq·g<sup>-1</sup> for Li<sup>+</sup>, 0.18 meq·g<sup>-1</sup> for Na<sup>+</sup>, and 0.10 meq·g<sup>-1</sup> for K<sup>+</sup>, Rb<sup>+</sup>, and Cs<sup>+</sup>, respectively. The  $pK_c$  value was nearly constant (2.9) for Li<sup>+</sup>/H<sup>+</sup> exchanges in the range below  $\bar{X}_{Li} < 0.5$  while it increased to 3.4 at  $\bar{X}_{Li} > 0.5$ . This indicates the presence of two types of adsorption sites with slightly different affinities for lithium ions. The  $pK_c$  values showed a tendency to increase with increasing  $\bar{X}_M$  for the other  $M^+$ /H<sup>+</sup> exchanges, probably due to an increase of negative surface charge with  $\bar{X}_M$ . The selectivity constant at  $\bar{X}_M = 0$  ( $pK_0$ ) could be estimated by extrapolating  $pK_c$  value to  $\bar{X}_M = 0$  (Table 1).

Figure 7 illustrates the  $pK_c$  vs.  $\bar{X}_{Li}$  plots in (LiCl+LiOH) and (KCl+LiOH) solutions. The  $pK_0$  values were nearly equal (2.9–3.2) regardless of the salt species and salt concentration (Table 1). In the range above  $\bar{X}_{Li} > 0.5$ , the  $pK_c$  value showed a tendency to decrease with increasing salt concentration. Since the decrease of  $pK_c$  in the (KCl+LiOH) system corresponds to the decrease of the pH with KCl concentration, the decrease may be partly due to the decrease of surface negative potential by the addition of neutral salt.

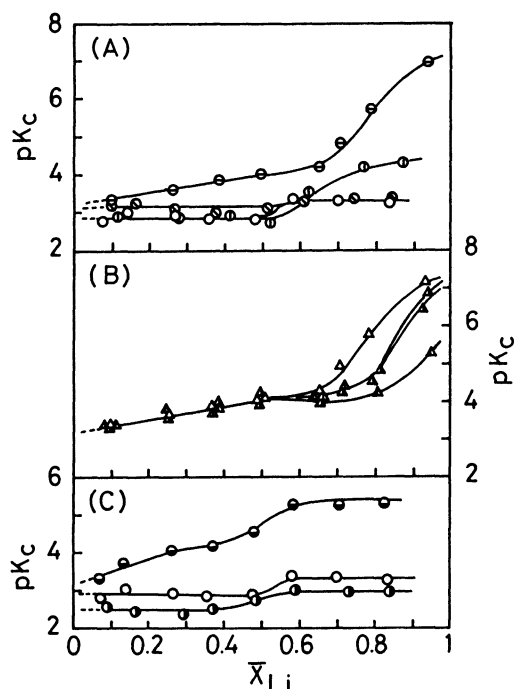


Fig. 7.  $pK_c$  vs.  $\bar{X}_{\text{Li}}$  plots. Figures 8(A), 8(B), and 8(C) are calculated from Figs. 2, 5, and 3, respectively. The symbols are the same as those in the corresponding figures.

Table 1. Values of  $pK_0$ ,  $pK$ , and  $\Delta G^\circ$  for  $\lambda\text{-MnO}_2$

System	Concentration of added salt $\text{mol dm}^{-3}$	$T$ $^\circ\text{C}$	$pK_0$	$pK$	$\Delta G^\circ$ $10^3 \text{ J mol}^{-1}$
LiCl+LiOH	0	25	3.23	4.53	25.9
	0.01	25	2.96	3.40	19.4
	0.1	25	2.91	3.13	17.9
	0.1	10	3.08	4.64	26.5
	0.1	40	2.58	2.74	16.4
KCl+LiOH	1	25	3.11	3.24	18.5
	0.03	25		4.33	24.7
	0.1	25	3.23	4.29	24.5
NaCl+NaOH	1	25		4.01	22.8
NaCl+NaOH	0.1	25	4.2	5.8	33
KCl+KOH	0.1	25	4.2	5.1	29
RbCl+RbOH	0.1	25	4.2	5.1	29
CsCl+CsOH	0.1	25	4.2	5.1	29

**Calculation of Equilibrium Constant.** The  $pK$  values calculated using Eq. 5 and the  $\Delta G^\circ$  values are given in Table 1. The  $\Delta G^\circ$  value for  $\text{Li}^+/\text{H}^+$  exchange showed tendencies to decrease with salt concentration and to decrease with adsorption temperature. The standard enthalpy and entropy changes ( $\Delta H^\circ$  and  $\Delta S^\circ$ ) at 298 K could be evaluated from the temperature dependence of  $\Delta G^\circ$  by the usual method. The  $\Delta H^\circ$  value, estimated with least square method, was 120 kJ per mole of lithium and a corresponding  $\Delta S^\circ$  300 J  $\text{K}^{-1} \text{ mol}^{-1}$ . Both of the  $\Delta H^\circ$  and  $\Delta S^\circ$  values

were positive and were larger than those of  $\text{Li}^+/\text{H}^+$  exchanges on another type of inorganic ion exchangers.<sup>22,23</sup> The positive  $\Delta G^\circ$  values may possibly arise from the increase of the volume of the unit cell and of water transfer to the aqueous solution from the exchanger with increasing adsorption of lithium ions at the tetrahedral vacant sites. Further study may be needed to determine the alternative contribution for  $\Delta S^\circ$  in this system.

## References

- 1) V. V. Vol'khin, G. V. Leont'eva, and S. A. Onorin, *Neorg. Mater.*, **9**, 1041 (1973).
- 2) G. V. Leont'eva and V. V. Vol'khin, *Zh. Prikl. Khim.*, **44**, 2615 (1971).
- 3) S. Xiang-mu and W. Xue-yuan, *Acta Chim. Sin.*, **39**, 711 (1981).
- 4) M. Tsuji and M. Abe, *Solv. Extr. Ion Exch.*, **1**, 97 (1984).
- 5) S. Xiang-mu and A. Clearfield, *J. Solid State Chem.*, **64**, 270 (1986).
- 6) K. Ooi, Y. Miyai, and S. Katoh, *Sep. Sci. Technol.*, **21**, 755 (1986). K. Ooi, Y. Miyai, and S. Kato, *Sep. Sci. Technol.*, **22**, 1779 (1987).
- 7) Y. Miyai, K. Ooi, and S. Katoh, Paper Presented at the 37th Meeting of Sea Water Science of Japan, Tokyo, June 1986.
- 8) J. C. Hunter, *J. Solid State Chem.*, **39**, 142 (1981).
- 9) K. Ooi, Y. Miyai, and S. Katoh, *Solv. Extr. Ion Exch.*, **5**, 561 (1987).
- 10) I. Tari and T. Hirai, *Denki Kagaku*, **52**, 498 (1984).
- 11) H. Tamura, M. Mitsuta, and M. Nagayama, *Denki Kagaku*, **54**, 250 (1986).
- 12) T. W. Healy, A. P. Herring, and D. W. Fuerstenau, *J. Colloid Interface Sci.*, **21**, 435 (1966).
- 13) J. W. Murray, *J. Colloid Interface Sci.*, **46**, 357 (1974).
- 14) L. S. Balistrieri and J. W. Murray, *Geochim. Cosmochim. Acta*, **46**, 1041 (1982).
- 15) M. Abe and T. Ito, *Nippon Kagaku Zasshi*, **86**, 1259 (1965).
- 16) M. Tsuji and M. Abe, *Bull. Chem. Soc. Jpn.*, **58**, 1109 (1985).
- 17) R. G. Burns and V. M. Burns, "Manganese Dioxide Symposium Vol. 2," ed by B. Schumm, Jr., H. M. Joseph, and A. Kozawa, MnO<sub>2</sub> Sample Office, Cleveland (1981), p. 97.
- 18) D. G. Wickham and W. J. Croft, *J. Phys. Chem. Solids*, **7**, 351 (1958).
- 19) J. B. Goodenough, M. M. Thackeray, W. I. F. David, and P. G. Bruce, *Rev. Chim. Minerale*, **21**, 435 (1984).
- 20) R. O. James, "Adsorption of Inorganics at Solid-Liquid Interface," ed by M. A. Anderson and A. J. Rubin, Ann Arbor Sci., Michigan (1981), p. 219.
- 21) G. L. Gaines, Jr. and H. C. Thomas, *J. Chem. Phys.*, **21**, 714 (1953).
- 22) A. Clearfield and D. A. Tuhtar, *J. Phys. Chem.*, **80**, 1302 (1976).
- 23) M. Abe and N. Furuki, *Solv. Extr. Ion Exch.*, **4**, 547 (1986).